

# Nanotubular Boron-Carbon Heterojunctions

Jens Kunstmann\* and Alexander Quandt

*Institut für Physik, Domstraße 10a, Ernst-Moritz-Arndt-Universität Greifswald, 17489 Greifswald, Germany*

(Dated: June 11, 2018)

Linear nanotubular boron-carbon heterojunctions are systematically constructed and studied with the help of *ab initio* total energy calculations. The structural compatibility of the two classes of materials is shown, and a simple recipe that determines all types of stable linear junctions is illustrated in some detail. Our results also suggest the compatibility of various technologically interesting types of nanotubular materials, leading to novel types of nanotubular compound materials, and pointing out the possibility of wiring nanotubular devices within heterogeneous nanotubular networks.

PACS numbers: 81.07.Lk, 81.07.De, 73.22.-f, 61.46.+w

## INTRODUCTION

Carbon nanotubes (CNTs) [1] have a number of fascinating properties, which could make them the material of choice for the future miniaturization of electronic devices: They are good thermal conductors, exhibit a good thermal resilience, are ductile and superb field emitters [2]. Furthermore their electronic properties range from metallic to semi-conducting, depending on their chiralities and radii [3].

Besides there are many other nanotubes made from inorganic materials [4, 5], like BN [6] or MoS<sub>2</sub> [7] nanotubes which have already been synthesized, or materials that have been predicted by theory like metal-boron nanotubes [8, 9] or the structurally related CaSi<sub>2</sub> nanotubes [10]. Another promising new type of nanotubular materials are nanotubes consisting of pure boron (B-nanotubes) [11, 12]. The stability and the mechanical properties of B-nanotubes (BNTs) would be quite similar to C- and BN-nanotubes, but all BNTs should be metallic, independent of their chirality [13]. Very recently Ciuparu *et al.* [14] successfully synthesized these nanotubes and thus confirmed the existence of BNTs, after similar efforts had already lead to the discovery of novel types of boron nanowires by various other groups [15, 16, 17, 18].

With such a large number of nanotubular systems available (a number which is very likely to further increase in the near future), possible nanotechnologies are most likely to be based on this *variety* of nanotubular materials rather than just CNTs (see [19, 20]). The functionalities of such *heterogeneous nanotubular networks* would mainly arise from their composite character.

But before one can seriously start any discussion about the future impact of heterogeneous nanotubular networks, it will be necessary to explore the stability of their key elements, first: the interfaces between different nanotubular materials. In the following, we will, for the first time, study the compatibility of different nanotubular materials in a *systematic fashion* by examining the structural and electronic properties of suitable model junctions between those systems.

To this end we decided to focus our studies on boron-

carbon nanojunctions, which may be seen as a structural paradigm for a large class of junctions, comprising most of the non-carbon based nanotubular materials mentioned above. On the basis of three exemplary structures, we will demonstrate the compatibility of CNTs and BNTs. Due to the exemplary character of the model junctions chosen for this study, our results also suggest the existence of similar junctions between a large number of related nanotubular materials.

## NANOTUBULAR HETEROJUNCTIONS

Nanotubes are geometrically constructed by rolling up a rectangular sheet that has been cut from a planar structure. For CNTs this planar structure will be the honeycomb lattice [3], while for BNTs the planar reference structure will be a (puckered) hexagonal lattice [13].

In order to approach the rather complex problem of heterogeneous nanotubular junctions we restricted our examinations to linear B-C junctions with constant chirality, where both parts of the junctions have similar radii. The sought B-C nanojunctions (and all other structures considered in this paper) are directly related to the structure of pure CNTs, as they can obviously be constructed from a single sheet. Therefore we may also classify them in a standard fashion employing a pair of integers (N,M) which specify the chiral vector  $\mathbf{C}_h = N\mathbf{b}_1 + M\mathbf{b}_2$ . Here  $\mathbf{b}_1$  and  $\mathbf{b}_2$  are basis vectors for a honeycomb lattice (see Fig.1).

Now the general prescription to create our sample B-C junctions goes as follows: A rectangular sheet is cut from a honeycomb lattice, such that its horizontal sides equal the chiral vector, and the vertical sides (dubbed *z*-direction in the following) being even multiples of a basic period, depending on the chirality of the tube [3]. An imaginary horizontal line in the middle of the sheet separates the upper and the lower part. The lower part consists of the original honeycomb lattice and is decorated with carbon atoms at each lattice site. The upper part is transformed into a hexagonal lattice after inserting another lattice point at the center of the honeycombs.

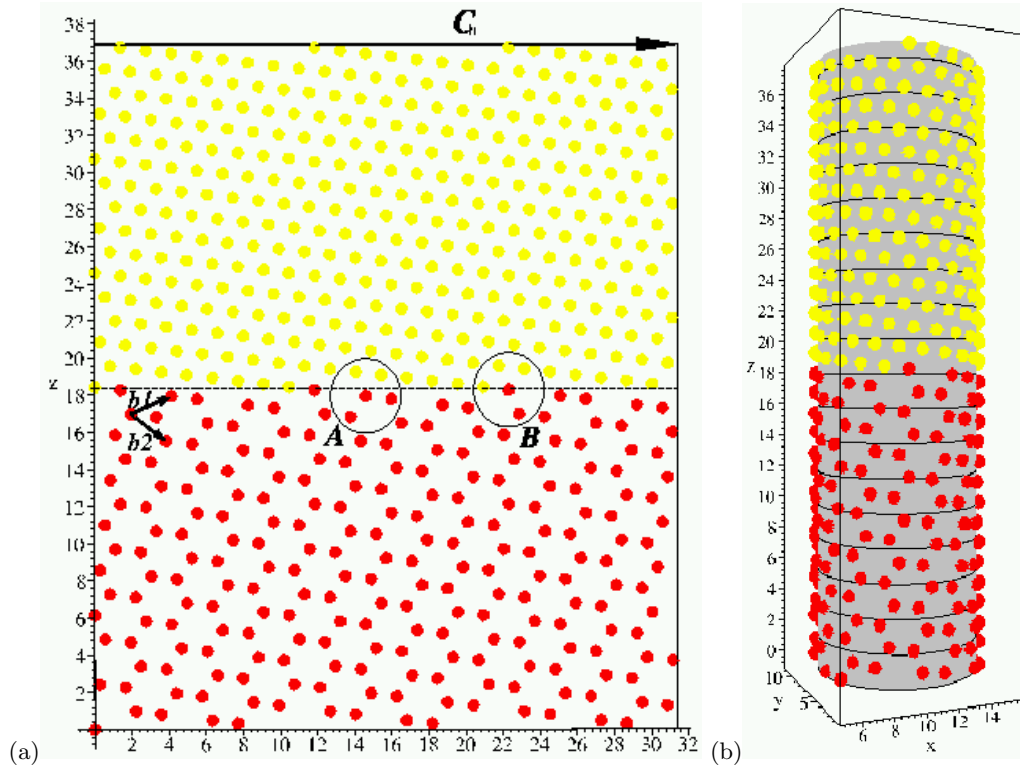


FIG. 1: Basic construction of B-C junctions. (a): (9,6) sheet, units are Å, light atoms are boron, dark atoms are carbon. Also indicated are the chiral vector  $C_h$  and the basis vectors of a honeycomb lattice  $b_1, b_2$ . The encircled parts emphasize the two structure elements  $A$  and  $B$  that appear in the transition region, and the dashed line separates the boron part from the carbon part. (b): chiral nanojunction constructed from (a) by rolling up the sheet and gluing it at the vertical sides, where the grey cylinder should emphasize the resulting tubular structure.

Next, this structure is decorated with boron atoms. Finally the sheet is rolled up and glued along its vertical sides (see Fig. 1).

For the stability of these junctions it will be crucial to understand the local atomic configurations close to the interface. Using the generation scheme described above, only two different structure elements, dubbed  $A$  and  $B$  in the following, may form close to the transition region (emphasized in Fig. 1). Thus a detailed study of the basic structural and chemical properties related to the formation of  $A$  and  $B$  will be sufficient to understand the stability of any linear and chiral nanojunction. These structure elements located around the interface regions will imply a planar coordination number of four for the constituent carbon atoms. Such coordinations are not found in pure CNTs, but higher planar coordinations of carbon atoms in contact with boron atoms have already been reported by Exner *et al.* [21] for small BC-clusters. We also note that non-chiral armchair and zigzag systems contain only one type of structure element  $A$  or  $B$ , and in order to be able to study their effects in a systematic fashion, we will restrict ourselves to armchair and zigzag types of nanojunctions.

## THEORETICAL METHODS

Due to its electron deficient character [22] boron has a complicated and versatile chemistry. The only theoretical tools that allow to describe its chemistry properly are first principles calculations [23].

In order to carry out *ab initio* type of simulations for nanotubular compound systems, we have to construct a solid composed of suitable unit cells containing those junctions. Within the  $xy$ -plane, we arrange the tubular junctions side by side on a hexagonal lattice of lattice constant  $a$ . Therefore we will simulate bundles (ropes) of linear junctions rather than single free-standing nanojunctions. In the  $z$ -direction we simply pile up our unit cells (with lattice constant  $c$ ). The whole procedure will lead to tubular structures that are a linear array of B-C and C-B transitions (see Fig. 2). Due to the periodic boundary conditions these systems can at best *approximate* single nanojunctions that would be present in the limit  $a, c \rightarrow \infty$ . Nevertheless the small approximants considered in this paper are sufficient to understand the properties of the structure elements  $A$  and  $B$ , as shown below.

The numerical calculations themselves were carried out

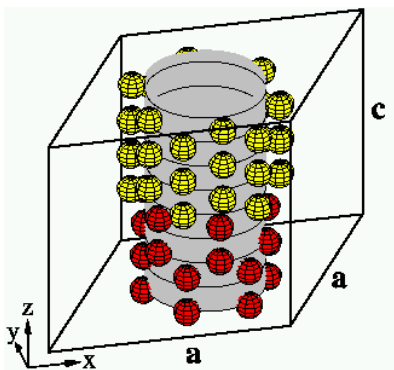


FIG. 2: The unit cell for hexagonal tubular bundles (ropes), with its lattice constants  $a$  and  $c$ , and the atomic decoration for the unrelaxed approximant Z1 (see text). Light atoms are boron, dark atoms are carbon and the grey cylinder again emphasizes the tubular structure of the junction.

using the VASP *ab initio* package, version 4.4.5 [24, 25]. The latter is a density functional theory (DFT) [26] based *ab initio* code using plane wave basis sets and a (super)cell approach to model solid materials. During all simulations, the electronic correlations were treated within the local-density approximation (LDA [27]), and the ionic cores of the system were represented by ultra-soft pseudopotentials [28]. With the help of the VASP program, one can determine interatomic forces and relax all degrees of freedom for a given decorated unit cell in order to detect atomic configurations which correspond to (local) minima on the total energy hypersurfaces. In order to perform these kinds of structure optimizations we employed a preconditioned conjugate gradient algorithm [29] and let *all* degrees of freedom relax, i.e. the complete set of atomic configurations as well as the unit cell parameters. The total energy as well as the  $k$ -point sampling were converged such that changes in the total energies were less than  $10^{-3}$  eV and interatomic forces were less than 0.05 eV/Å.

It turned out that the energy hypersurfaces of our structures were rather complex and full of local minima. In order to approach the most stable structures, we developed a procedure where the starting configurations were prerelaxed with lower numerical precision until a (local) minimum was found, and afterwards we continued the relaxations with optimal precision. A reduced precision leads to somewhat imprecise interatomic forces, but we found that such a procedure would result in the scanning of the energy hypersurface over a wider range.

In the following, we will discuss our results for the following types of model junctions: Armchair 1 (A1) and Armchair 2 (A2) approximate an armchair (6,6) junction, and Zigzag 1 (Z1) approximates a zigzag (6,0) junction (Fig. 4). Besides (6,6) and (6,0) BNTs and CNTs have been relaxed, which are considered as suitable reference systems (Fig. 3).

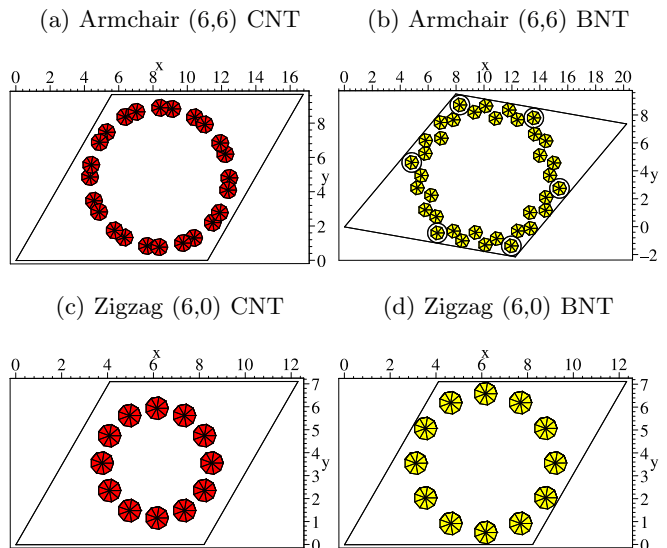


FIG. 3: Top view of the (relaxed) reference structures placed around the center of their unit cells. Encircled atoms in (b) have additional covalent bonds to neighboring nanotubes on the superlattice. Units are Å, light atoms are boron and dark atoms are carbon.

A1 was prerelaxed with the Brillouin zone being sampled by just the central  $\Gamma$ -Point, and finished with a  $4 \times 4 \times 4$  grid. A  $4 \times 4 \times 4$  grid was used to finish Z1, with smaller FFT-grids and a smaller plane wave basis set to do the prerelaxation. Finally A2 was prerelaxed with the  $\Gamma$ -Point, only and finished with a  $2 \times 2 \times 2$  grid. The (6,0) CNT was relaxed with a  $4 \times 4 \times 7$  grid and the total energy was calculated on a  $5 \times 5 \times 7$  grid. The armchair (6,6) CNT was prerelaxed with  $4 \times 4 \times 6$  and finished with  $5 \times 5 \times 9$ . The boron (6,0) zigzag nanotube was started with  $3 \times 3 \times 5$  and finished with  $5 \times 5 \times 11$   $k$ -points. The relaxed armchair BNT structure was obtained from [8], where it was relaxed on a  $7 \times 7 \times 7$  grid. The cutoff energy for the expansion of the wave function in plane waves was 286.6 eV for A2, 358.2 eV for A1, Z1 and the CNTs, and 321.4 eV for the BNTs.

The cohesive energy of each structure (Tab. I) was calculated by dividing the binding energy per unit cell by the number of atoms contained within that unit cell. In order to judge the stability of our model junctions, we decided to compare the cohesive energies of the relaxed structures to a reference cohesive energy of a phase-separated system of pure CNTs and pure BNTs of the same structure type, see Table I. For the (6,6)-junction the reference binding energy would be  $E_{\text{bind}}^{\text{ref}} = 24 \times 10.023 + 36 \times 7.004 = 492.696$  eV, and the corresponding reference cohesive energy would be  $E_{\text{coh}}^{\text{ref}} = E_{\text{bind}}^{\text{ref}}/60 = 8.212$  eV/atom. All cohesive energies as well as energetic differences with respect to the reference cohesive energies are given in table I.

TABLE I: Structure data and energies for nanojunctions and reference structures. (N,M): nanotube structure type, C: number of carbon atoms per unit cell, B: number of boron atoms per unit cell, (a,c): lattice constants  $a$  and  $c$  of unit cell in Å,  $a_{C-C}$ ,  $a_{B-B}$ ,  $a_{B-C}$ : range of bond lengths in Å of C-C, B-B, and B-C bonds, respectively,  $E_{\text{coh}}$ : cohesive energies in eV/atom,  $E_{\text{coh}}^{\text{ref}}$ : reference cohesive energy in eV/atom (see text).

System	(N,M)	C	B	(a,c)	$a_{C-C}$	$a_{B-B}$	$a_{B-C}$	$E_{\text{coh}}$	$E_{\text{coh}}^{\text{ref}}$	$E_{\text{coh}}^{\text{ref}} - E_{\text{coh}}$
Armchair 1 (A1)	(6,6)	24	36	(12.06,5.54)	1.40 ... 1.45	1.65 ... 1.85	1.53 ... 1.57	8.079	8.212	0.13
Zigzag 1 (Z1)	(6,0)	24	36	(8.32,8.95)	1.40 ... 1.45	1.61 ... 1.96	1.48 ... 1.74	7.964	8.038	0.07
Armchair 2 (A2)	(6,6)	36	84	(11.93,10.70)	1.40 ... 1.45	1.58 ... 1.95	1.49 ... 1.72	7.839	7.910	0.07
C-Nanotube	(6,6)	24	—	(11.17,2.45)	1.41	—	—	10.023	—	—
B-Nanotube	(6,6) <sup>a</sup>	—	36	(12.42,2.84)	—	1.58 ... 1.86	—	7.004	—	—
C-Nanotube	(6,0)	24	—	(8.20,4.22)	1.39 ... 1.43	—	—	9.791	—	—
B-Nanotube	(6,0)	—	12	(8.18,1.65)	—	1.65 ... 1.78	—	6.870	—	—

<sup>a</sup>relaxed structure from [8]

## RESULTS

Our survey started with the relaxation of the reference structures, which are bundles (ropes) of pure CNTs and BNTs. They are displayed in Fig. 3 (top view). While the surface of small radius CNTs is always smooth (Fig. 3a,c), BNTs *can* exhibit a puckered surface [13], which shows up in Fig. 3b, but not in Fig. 3d. Due to higher B-B bond lengths, the average radius of a BNT is always bigger than the radius of a CNT of the same structure type. Another major difference between CNTs and BNTs is the potential of the latter to form covalent intertubular bonds [8]. In contrast, the CNTs may only bind to each other via van der Waals types of interactions [3]. Such covalent bonds are indeed present in the model (6,6) BNT, and the atoms that form these bonds are encircled in Fig. 3b. The coordination number of boron atoms in BNTs is usually six [30] or even seven for atoms forming intertubular bonds, and it is always three in CNTs. The range of bond lengths, the parameters of the unit cells, and the cohesive energies of all fully relaxed structures can be found in table I.

The relaxed approximants A1, A2, and Z1 as well as the initial configurations are shown in planar view in Fig. 4. The left column shows the sheet, from which we constructed the starting configurations. In the middle the optimized junctions were projected back onto a similar sheet. The right column shows the junctions and their unit cells in top view. All of these structures have a  $C_6$ -Symmetry, e.g. they may be dissected into six identical 60°-wedges (indicated by dashed lines in the planar views)[31].

The cohesive energies of all approximants are below the cohesive energies of the corresponding phase-separated reference systems (see Tab. I). But the systems of isolated BNTs and CNTs are only slightly more stable than the junctions presented in this study. Each junction on the superlattice will bind to neighboring tubes via covalent boron atoms. There are no covalent intertubular bonds involving carbon. Instead, the carbon part of the

junctions almost rigidly stays in its initial geometry, and generally leads to smooth surfaces for the carbon part of the junctions. The boron on the other hand turns out to be more flexible, always forming puckered surfaces.

We studied the properties of structure element *A* by setting up the approximants A1. The cohesive energy of A1 lies 0.13 eV/atom below its cohesive reference energy, making this system slightly less stable than the phase separated reference system. After relaxation the hexagonal symmetry of the boron part has disappeared, and the junction was transformed into a new structure with 4-fold intratube coordination for boron, and 3-fold coordination for carbon (see Fig 4b). It seems that carbon tends to retain the planar  $sp^2$ -environment and forces the boron atoms into an unusual quasiplanar arrangement with rather low coordination numbers.

To overcome the somewhat constrained arrangements of A1, we set up another approximant (not shown) chosen to be twice as long in the  $z$ -direction, and comprising twice as many atoms, but still containing structure element *A*, only. The relaxed structure had the same structural problems as A1 and was almost isoenergetic to A1. This gives a consistent picture and certainly shows that the structural problems encountered for these types of armchair approximants are no artefacts of small unit cells. Thus the starting geometries involving the structure element *A* are obviously far from optimal.

In a next step we studied the structure element *B* by surveying approximant Z1. Its cohesive energy lies just 0.07 eV/atom below the reference energy. The planar view in Fig. 4e looks almost identical to its starting configuration and the basic lattice structures in both parts of the junction are maintained, allowing for high coordination numbers of the constituent atoms. It seems as if this type of heterojunction could be formed by sticking together two perfect zigzag tubes. It therefore looks as if nanotubular junctions formed with structure element *B* are generally favorable.

Therefore we tried to incorporate *B* in junctions of armchair type as well. To this end, one has to mod-

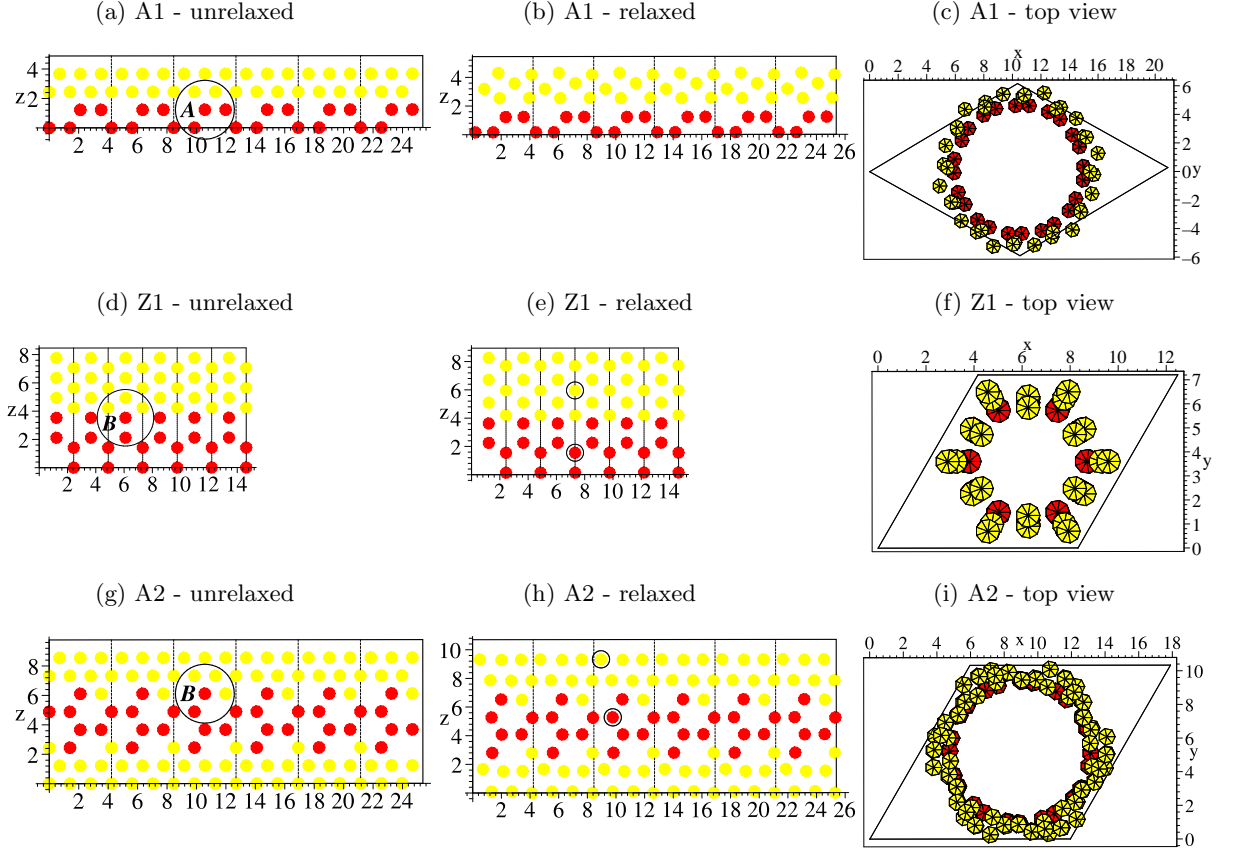


FIG. 4: First column: starting geometries in planar view, encircled parts emphasize the structure elements *A* and *B*. Dashed lines indicate six similar wedges partitioning the unit cells. Second column: relaxed structures in planar view. The local density of states of the encircled atoms in (e) and (h) is plotted in Fig. 5. Third column: top view of relaxed structures in their unit cells. Units are in Å, and light atoms are boron, and dark atoms are carbon.

ify the construction scheme and allow for a mixing of the species at the interface. Such a scenario has been realized in approximant A2 (Fig. 4, third line). The unit cell has been shifted by  $c/4$ . Now the two transition regions in every unit cell are clearly visible. The relaxed junctions shows properties very similar to Z1. Its cohesive energy is 0.07 eV/atom below the reference energy. Again the planar view in Fig. 4h looks almost identical to its initial configuration, indicating a starting point on the energy hypersurface very close to the sought minimum. Though very different in geometry Z1 and A2 exhibit very similar properties: the same stability, the same mean coordination number and the same mean number of intertubular bonds.

Finally we would like to discuss the basic electronic properties of Z1 and A2. The first line of Fig. 5 shows the total electronic density of states (DOS) of the structures near the Fermi energy  $E_F$ . The double-plots allow for a comparison of the local DOS of a central C- or B-atom (these atoms are encircled in Fig. 4e and 4h)[32] to the DOS of the reference systems, which are considered as bulk. Both are very different. Thus the

approximants obviously do not contain bulk states and the transition to the bulk proceeds over wider ranges, which cannot be simulated by the small approximants presented in this study. The position of major van-Hove-peaks and band gaps in the local DOS is homogeneous throughout the junction (thus it does not differ in the local and total DOS). This could be an indication for a common  $\pi$ -electron system extending throughout the junction. Finally we also found that the total DOS looks more similar to the local DOS of the boron atom rather than to the local DOS of carbon.

## CONCLUSIONS

For the first time we explored the stability, geometry and basic chemical and electronic properties of sample carbon-boron heterojunctions.

Starting from a general prescription to generate linear nanotubular junctions with arbitrary radius and chirality we showed that only two structure elements *A* and *B* can appear at the B-C transition of such a junction.

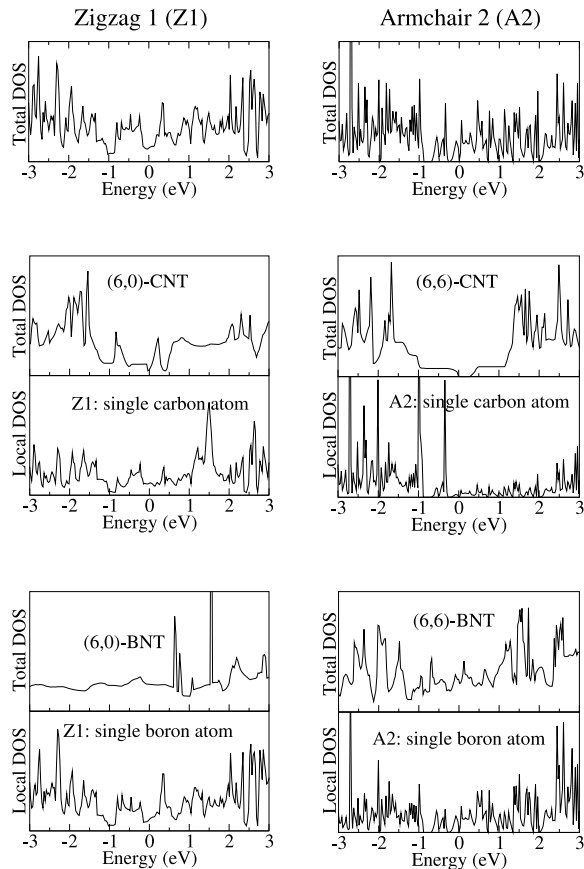


FIG. 5: Total and local density of states (DOS) in arbitrary units of Z1 and A2 (first and second column, respectively). In the split-panels we compare the total DOS of the reference structures (bulk) (see Fig. 3) to local DOS of atoms within the junctions. These atoms are encircled in Fig. 4e and 4h.  $E = 0$  equals the Fermi energy  $E_F$ .

The general atomic arrangements of *A* and *B* look rather similar, but in *A* the central carbon atoms will bind to two boron and two carbon atoms, whereas for *B* the central carbon atom will bind to three boron and one carbon atom, only.

We then studied the properties of *A* and *B* independently by examining approximants for a (6,6) armchair and a (6,0) zigzag junction. From a structural point of view, the carbon part of all relaxed junctions looks rather similar to what is known for stand-alone carbon nanotubes - exhibiting a smooth surface and preferring carbon in a 3-fold coordinated environment [3]. The boron part of the junctions is always puckered and forms intertubular bonds, as known from stand-alone boron nanotubes [11, 30], but the ideal hexagonal arrangement in the boron part of the junctions is only preserved by junctions that feature the structure element *B*. Such systems have similar properties; they display the same average coordination numbers, the same types of intertubu-

lar bonds, and they are only 0.07 eV/atom less stable than a phase separated system of carbon and boron nanotubes. Junctions that feature element *A* have structural problems and their formation energies per atom are approximately twice as high as for junctions formed with element *B*.

The central carbon atom of structure element *B* is 4-fold coordinated. Besides the known tetragonal  $sp^3$  arrangements, we found new planar and quasiplanar atomic arrangements induced by the electron deficiency of boron [22]. Such forms have not been reported in solid system before and are in partial agreement with results found by Exner *et al.* [21], who studied small planar BC-clusters.

The analysis of the total and local electronic DOS indicates that all junctions consist of interface states, only. A transition towards the bulk will proceed over wider ranges than those that were studied here. Furthermore there are indications for a common  $\pi$ -electron system extending throughout the whole junction.

After relaxation all approximants were still tubular, had distinct boron and carbon parts and showed a clear B-C interface. This itself is a strong indication for the compatibility of these two nanotubular materials. In detail, it seems that structure element *B* is the key to generate optimal zigzag and armchair junctions, and those results also suggest that *any* stable linear and chiral nanotubular B-C junction may be formed by building structure elements *B* within the transition region. The relative instability of 0.07 eV/atom for the apparently optimal model junctions is surprisingly small, considering that at the interface both the boron and the carbon lattices are significantly disturbed, and second, that our approximants are really small. This energy barrier can be overcome thermodynamically, and it is very likely to decrease further for bigger systems. The influence of lattice perturbations is apparent in A1, where only small dislocations of the boron atoms give rise to a doubling of the relative instability. We thus conjecture that heterogeneous junctions between boron and carbon nanotubes should be possible. Our study also clarifies the *local* chemistry at the interface of B-C junctions, which could be shown to be independent of the periodic boundary conditions.

Finally, we hope that further studies of suitable model systems similar to the structures presented in this study will shed some light on the formation and stability of other nanotubular heterojunctions and networks. According to our studies nanotubular carbon and boron materials seem to be compatible, and given the large number of structurally related materials (see introduction), our results also suggest the possibility of a large variety of novel heterogeneous nanotubular materials forming extended network systems. By taking advantage of the fortunate structural and electronic properties of heterogeneous nanotubular systems, one might even hope for the development of novel compound nanotubular devices in the future.

## ACKNOWLEDGMENTS

The authors thank Dr. Sylvio Kosse (Greifswald) for technical support during our extensive use of the 'snowwhite' computer cluster, and Dr. Ihsan Boustani (Wuppertal) and Prof. Klaus Fesser (Greifswald) for various helpful discussions.

---

\* Electronic address: kunstmann@physik.uni-greifswald.de

- [1] S. Iijima, *Nature* **354**, 56 (1991).
- [2] P. Collins and P. Avouris, *Sci. Am. (Int. Ed.)* **238**(6), 62 (2000).
- [3] M. S. Dresselhaus, G. Dresselhaus, and P. Eklund, *Science of Fullerenes and Carbon Nanotubes* (Academic Press, San Diego, 1996).
- [4] W. Tremel, *Angew. Chem. Int. Ed.* **38**, 2175 (1999).
- [5] R. Tenne and A. K. Zettl, in *Carbon Nanotubes* (Springer-Verlag, New York, 2001), pp. 81–112.
- [6] N. G. Chopra, R. J. Luyken, K. Cherrey, V. H. Crespi, M. L. Cohen, S. G. Louie, and A. Zettl, *Science* **269**, 966 (1995).
- [7] R. Tenne, L. Margulis, M. Genut, and G. Hodes, *Nature* **360**, 444 (1992).
- [8] A. Quandt, A. Y. Liu, and I. Boustani, *Phys. Rev. B* **64**, 125422 (2001).
- [9] P. Zhang and V. H. Crespi, *Phys. Rev. Lett.* **89**, 56403 (2002).
- [10] S. Gemming and G. Seifert, *Phys. Rev. B* **68**, 75416 (2003).
- [11] I. Boustani and A. Quandt, *Europhys. Lett.* **39**, 527 (1997).
- [12] A. Gindulyte, N. Krishnamachari, W. N. Lipscomb, and L. Massa, *Inorg. Chem* **37**, 6546 (1998).
- [13] I. Boustani, A. Quandt, E. Hernandez, and A. Rubio, *J. Chem. Phys.* **110**, 3176 (1999).
- [14] D. Ciuparu, R. F. Klie, Y. Zhu, and L. Pfefferle, *J. Phys. Chem. B* **108**, 3967 (2004).
- [15] L. Cao, Z. Zhang, L. Sun, C. Gao, M. He, Y. Wang, Y. Li, X. Zhang, G. Li, J. Zhang, et al., *Adv. Mater.* **13**, 1701 (2001).
- [16] Y. Wu, B. Messer, and P. Yang, *Adv. Mater.* **13**, 1487 (2001).
- [17] C. J. Otten, O. R. Lourie, M. Yu, J. M. Cowley, M. J. Dyer, R. S. Ruoff, and W. E. Buhro, *J. Am. Chem. Soc.* **124**, 4564 (2002).
- [18] Y. Zhang, H. Ago, M. Yumura, T. Komatsu, S. Ohshima, K. Uchida, and S. Iijima, *Chem. Commun.* **23**, 2806 (2002).
- [19] L. Chico, V. H. Crespi, L. X. Benedict, S. G. Louie, and M. L. Cohen, *Phys. Rev. Lett.* **76**, 971 (1996).
- [20] Z. Yao, H. W. C. Postma, L. Balents, and C. Dekker, *Nature* **402**, 273 (1999).
- [21] K. Exner and P. von Ragué Schleyer, *Science* **290**, 1937 (2000).
- [22] L. Pauling, *Nature of the chemical bond* (Cornell University Press, Ithaca, 1960).
- [23] I. Boustani, *Phys. Rev. B* **55**, 16426 (1997).
- [24] G. Kresse and J. Furthmüller, *Comput. Mater. Sci.* **6**, 15 (1996).
- [25] G. Kresse and J. Furthmüller, *Phys. Rev. B* **54**, 11169 (1996).
- [26] W. Kohn and L. Sham, *Phys. Rev. B* **140**, 1133 (1965).
- [27] D. Ceperley and B. Alder, *Phys. Rev. Lett.* **45**, 566 (1980).
- [28] D. Vanderbilt, *Phys. Rev. B* **41**, 7892 (1990).
- [29] M. P. Teter, M. C. Payne, and D. C. Allan, *Phys. Rev. B* **40**, 12255 (1989).
- [30] I. Boustani and A. Quandt, *Comput. Mater. Sci.* **11**, 132 (1998).
- [31] This  $C_6$ -Symmetry is generated by the six-fold symmetry of the hexagonal tubular superlattice as well as the structure types of the reference nanotubes, which are either (6,6) or (6,0).
- [32] Due to the  $C_6$ -Symmetry the local DOS of similar atoms within different wedges are (almost) identical, while non-equivalent atoms differ significantly.